RSC Advances

RSC Advances

www.rsc.org/advances

ROYAL SOCIETY OF CHEMISTRY

www.rsc.org/advances

RSC Advances

ARTICLE TYPE

Ni(OH)₂@Cu dendrite structure for highly sensitive glucose determination

Hyeri Jung, Sang Ha Lee, Jiao Yang, Misuk Cho, and Youngkwan Lee*

Fast and accurate monitoring of glucose level in various fields has attracted increasing attention in recent years. In this study, a nickel hydroxide-coated copper dendrite structure [Ni(OH)₂@Cu] was prepared by a facile two-step electrodeposition on gold substrate and was used as a non-enzymatic glucose sensor. The surface morphology of the Ni(OH)₂@Cu dendrite structure was characterized by scanning

10 electron microscopy and elemental mapping, and its composition was confirmed by X-ray diffraction and X-ray photoelectron spectroscopy. Due to the large surface area of the dendrite structure, the as-prepared sensor demonstrated a high electrocatalytic activity towards the oxidation of glucose in alkaline solution. Following analysis of the optimum deposition and sensing conditions, the developed sensor showed a high sensitivity of 2082 $\mu AmM^{-1}cm^{-2}$ over a wide linear range of 1- 4500 μM, as well as a low detection limit of 0.24 μM (S/N=3) with a rapid response time of 2 s. This sensor can also reliably measure glucose concentration in human urine

15 samples, indicating its use as a promising glucose sensor.

1. Introduction

The fast, reliable, and highly sensitive determination of glucose has attracted considerable interest in various fields, such as

20 biochemistry, clinical diagnostics, and the food industry [1]. The electrochemical method is a powerful, simple, and low-cost technique for glucose sensing [2]. Enzymatic glucose sensors based on the immobilization of glucose oxidised on various substrates are the topic of most previous studies. However, these conventional

25 enzymatic sensors usually suffer from short device lifetime and activity decay because enzymatic glucose is easily affected by temperature, pH, humidity, and toxic chemicals [3].

To overcome these disadvantages, a non-enzymatic glucose sensor is an attractive alternative technique. In the past several years, non-

30 enzymatic glucose sensors have received much attention due to their high sensitivity, excellent stability, low production cost, and promising response speed [4-5]. Various metals (Pt, Pd, Cu, and Ni) have been explored as electrode materials for glucose detection [6-9].

35 Noble metal electrodes show high sensitivity and good stability for electro-analysis, but the cost is excessive. For Cu and Ni electrodes, low sensitivity and poor stability due to ease of oxidation in air and solution may limit their practical applications [10, 11]. However, transition metal oxides (Cu$_x$O, NiO, MnO₂, etc.)

40 [12-14] or metal hydroxides (Ni(OH)₂, Cu(OH)₂, etc.) [15,16] are of great interest and display many advantages for non-enzymatic glucose sensing such as fast response, high sensitivity, low detection limit, good stability, and low cost.

Among various transition metal-based electrodes, nickel

45 hydroxide [Ni(OH)₂] is an attractive material due to its excellent electroactivity, low cost, and environmentally benign properties. Numerous efforts have been devoted to the synthesis of Ni(OH)₂ with various morphologies, such as nanospheres, hollow nanoboxes, and nanoplates [10, 15, 17], which have the advantages

50 of high surface area and novel size effect. Ni(OH)₂-based sensors have excellent electro-catalysis for glucose due easy deoxidation of the NiOOH in the redox pair of Ni(OH)₂/NiOOH [18]. However, nanoscale electrode materials are difficult to prepare and have poor stability, which can be problematic for extended oxidation periods

55 under an applied potential.

Based on these findings, a dendritic structure consisting of a main stem and numerous side branches has received significant attention in catalysis and technological fields [19, 20]. The large surface area, short diffusion length, and mechanical integrity of the dendrite can

60 provide both an extraordinarily high activated surface and robust stability resulting from the micro- and nano-sized assemblies [21-23]. To synthesize a metal dendrite directly on a conductive substrate, electrodeposition can be easily employed without any post-treatment. Qiu et al. prepared a dendritic copper structure by

65 electrodeposition, and the modified electrode showed strong electroreduction ability for hydrogen peroxide and nitrate sensing [24]. Lin's group electrodeposited gold dendrites in the presence of

cysteine, which had a good electro-oxidation effect for methanol [25].

Here, we report a novel $Ni(OH)_2@Cu$ dendrite fabricated by a facile two-step electrodeposition process. $Ni(OH)_2$ as an electro-active sensing material is difficult to directly prepare as a dendrite structure with controllable shape and size using an electrochemical method. Hence, a Cu dendrite was initially electrodeposited on a gold substrate, which served as a template for $Ni(OH)_2$ electrodeposition. The morphology and thickness of $Ni(OH)_2$ were controlled by the applied current and deposition time, respectively. The nano/micro dendritic structures are expected to highly promote electron transfer in glucose oxidation and to show high biocompatibility between glucose and the electrode surface, resulting in short response time, high sensitivity, and long-term stability. The dendrite electrode was utilized to investigate the electrocatalytic oxidation of glucose with a high sensitivity (2082 $\mu AmM^{-1}cm^{-2}$), wide linear range (1 - 4500 μM), good selectivity, and repeatability. The practical application of this sensor was further tested by determining the glucose concentration in real human urine samples.

2. Experimental

Experimental Materials

Copper (II) chloride, potassium nitrate, potassium hexacyanoferrate (II) trihydrate, potassium hexacyanoferrate (III), potassium chloride, urea, aspartic acid (AP), ascorbic acid (AA), dopamine (DP), uric acid (UA), and d-(+)-glucose were purchased from Aldrich Chemical Co. (USA). Sulfuric acid (95 %), 0.1 M sodium hydroxide, and nickel (II) nitrate hexahydrate were purchased from SAMCHUN PURE CHEMICAL Co. (KOREA). All materials were used as received.

Preparation of Cu dendrite on gold substrate

Gold plate (surface area = 0.28 cm^2) was pre-treated according to the literature [26]. The dendrite morphology could be tuned by altering potential, temperature, and precursor-concentration. Cu dendrite was electrochemically deposited on the gold substrate by chronoamperometry (CA) at a potential of -0.5 V for 5 min in aqueous solution containing 0.15 M $CuCl_2$ and 0.75 M H_2SO_4 (pH=2.7) [27].Under this conditions, uniform and microsized Cu dendrite was obtained. Finally, the Cu dendrite modified gold electrode was washed with DI water and dried at room temperature.

Electrodeposition of $Ni(OH)_2$ on Cu dendrite

The deposition of $Ni(OH)_2$ on Cu dendrite was carried out by chronopotentiometry (CP) at -0.1 $mAcm^{-2}$ for 10 min in 0.1 M $Ni(NO_3)_2 \cdot 6H_2O$ + 0.1 M KNO_3 aqueous solution. The thickness of $Ni(OH)_2$ was controlled by the deposition time and current. The obtained $Ni(OH)_2@Cu$ dendrite was washed with DI water and dried in vacuum oven at room temperature for 2 h. For comparison, $Ni(OH)_2$ film was also prepared on gold substrate under the same conditions. The both loading masses of $Ni(OH)_2$ were held at 0.01 mg.

Characterizations

The morphology of the $Ni(OH)_2@Cu$ dendrite was characterized by a scanning electron microscope (SEM, JEOL JSM-7000F, Japan) with an accelerating voltage of 15 kV. Energy-dispersive X-ray spectroscopy (EDX, JEOL JSM-7000F, Japan) was used for elemental analysis of the sample. The composition of $Ni(OH)_2@Cu$ dendrite was identified by HP-thin film X-ray diffraction measurements (XRD, Bruker, Germany) with a Cu K target (λ = 1.54056 A) a n d X-ray photoelectron spectroscopy (XPS, ESCA2000, VG microtech, England). All electrochemical experiments were performed o n a potentiostat (VSP, Princeton Applied Research, USA) using a three electrode system: the modifi ed electrodes, a platinum plate and an Ag/AgCl (saturated KCl) as working, counter, a n d reference electrode, respectively. Electrochemical impedance spectroscopy (EIS) were measured in 0.1 M KCl containing 5 mM $[Fe(CN)_6]^{3-/4-}$ in the frequency range of 100 mHz −100 kHz (28). The Z SimpWin EIS DATA analysis software (Perkin-Elmer, Version 2.00) was used to analyze the obtained EIS data and fit an equivalent circuit. At least 5 test specimens were measured to obtain the average R_{et} and C value. Cyclic voltammetry (CV) and Chronoamperometry (CA) were executed in a 0.1 M NaOH solution under stirred conditions. HPLC analysis was performed using Dionex ICS-5000 HPLC system (Dionex Corporation, MA, USA) equipped with Carbopac™ PA-1 guard (250x4 mm column, Dionex Corporation, MA, USA) at 25 ºC and an electrochemical detector using Au, Ti, and pH-Ag/AgCl as working, counter, and reference electrodes, respectively. Glucose concentrations from HPLC-amperometry were calculated by integrating the area under designated peaks and standard calibration curves. Error bars represent the relative standard deviation of triplicate measurements unless otherwise noted [29].

3. Results and discussion

Characterization of the $Ni(OH)_2@Cu$ dendrite electrode

The $Ni(OH)_2@Cu$ dendrite structure was successfully prepared by a facile two-step electrodeposition process. A Cu dendrite structure was first electrodeposited on gold substrate by chronoamperometry (CA); it then served as a template for subsequent electrodeposition of a thin $Ni(OH)_2$ film. Figure 1A shows the SEM image of the hierarchical structure of Cu dendrite obtained using electro-deposition. The prepared Cu dendrite has a main stem from which many side branches grow out. The SEM image of Figure 1B details the morphology of a typical dendrite. The primary stem (marked with an arrow) were ca. 10 μm with a diameter of ca. 0.3 μm, and the secondary branches ranged from 0.1 to 2 μm with a diameter of ca. 0.3 μm. The morphology of the $Ni(OH)_2@Cu$ dendrite was controlled by the deposition time and applied current. The structures of the $Ni(OH)_2$ Cu dendrites created with different deposition times and applied currents are presented in Fig. S1 (Supplementary Materials). The result shows that, when $Ni(OH)_2$ was deposited at -0.1 $mAcm^{-2}$ for 10 min, a uniform $Ni(OH)_2$ thin film completely covered the Cu dendrite surface without any aggregation. As shown in Fig. 1C and D, the dendritic structure of $Ni(OH)_2@Cu$ was well maintained after the $Ni(OH)_2$ coating, and the thickness of the branches was slightly increased.
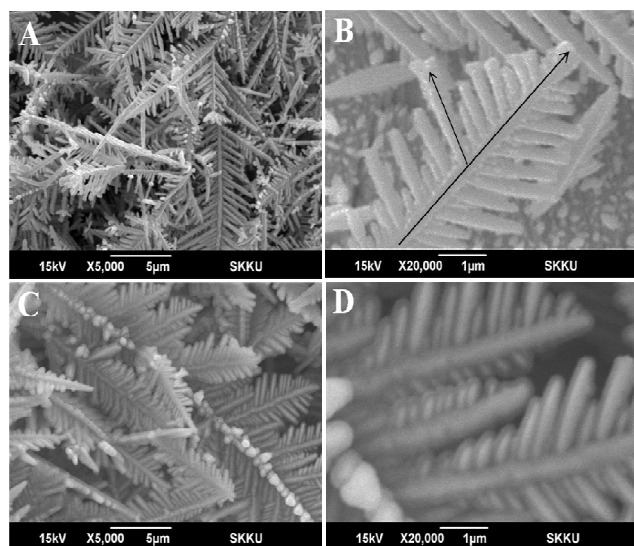
Fig.1

SEM images of Cu dendrite (A), high magnification (B), Ni(OH)$_2$ @ Cu dendrite (C) and high magnification (D)

We believe that the retained dendrite structure not only provides an extraordinarily highly activated surface, but also possesses robust stability imparted from the micro- and nano-sized assemblies [30]. EDX mapping results (Fig. S2) further illustrated that the Ni(OH)$_2$ was homogeneously distributed throughout the entire dendrite.

X-ray photoelectron spectroscopy (XPS) was investigated to measure the binding energy, from which we could estimate the various chemical states of bonded elements. The survey spectrum for the formation of Ni(OH)$_2$ @ Cu dendrite showed in Fig. 2A

In the Ni 2p region (Fig. 2B), the first peak at 856.9eV was associated with Ni(OH)$_2$. At higher energies, additional densities were detected in accordance with two peaks: a shake-up peak corresponding to Ni(OH)$_2$ (862.4 eV) and a β-NiOOH $^{2+}$ portion (867.5 eV). This is in good agreement with the peak positions reported by others [31-33]. In the O 1s high-resolution spectrum, the oxygen envelope was fitted with two peaks at 532.3 and 533.2 eV (Fig. 2C). The first peak is attributed to hydroxide groups (-OH), and the second corresponds to metal-oxygen species [34]. These results indicate that Ni(OH)$_2$ can be successfully deposited on a Cu dendrite by a simple electrochemical method. The XRD patterns for Cu dendrite and Ni(OH)$_2$@Cu dendrite were presented in Fig. S3. Metallic nature of Cu dendrite was found with characteristic peaks at 2θ = 42.74∘, 49.53∘, and 72.56∘, which were related to Cu(111), (200), and (220), respectively. After the Ni(OH)$_2$coating, there was no characteristic peaks of crystalline Ni(OH)$_2$ indicating the amorphous structure of Ni(OH)$_2$. The result was the same as those obtained by others [15, 32].

The electrochemical properties of the Ni(OH)$_2$@Cu dendrite electrode were characterized using EIS responses. The impedance spectra were recorded for bare gold, Ni(OH)$_2$ film, and Ni(OH)$_2$@Cu dendrite using a modified equivalent circuit (Fig. 3). The bare gold and Ni(OH)$_2$@Cu dendrite electrode exhibited a nearly straight line in the Nyquist plot of impedance spectroscopy (Fig. 3, curves a and c), indicating that a diffusion-limited electron-transfer process was dominant for the frequency range explored.
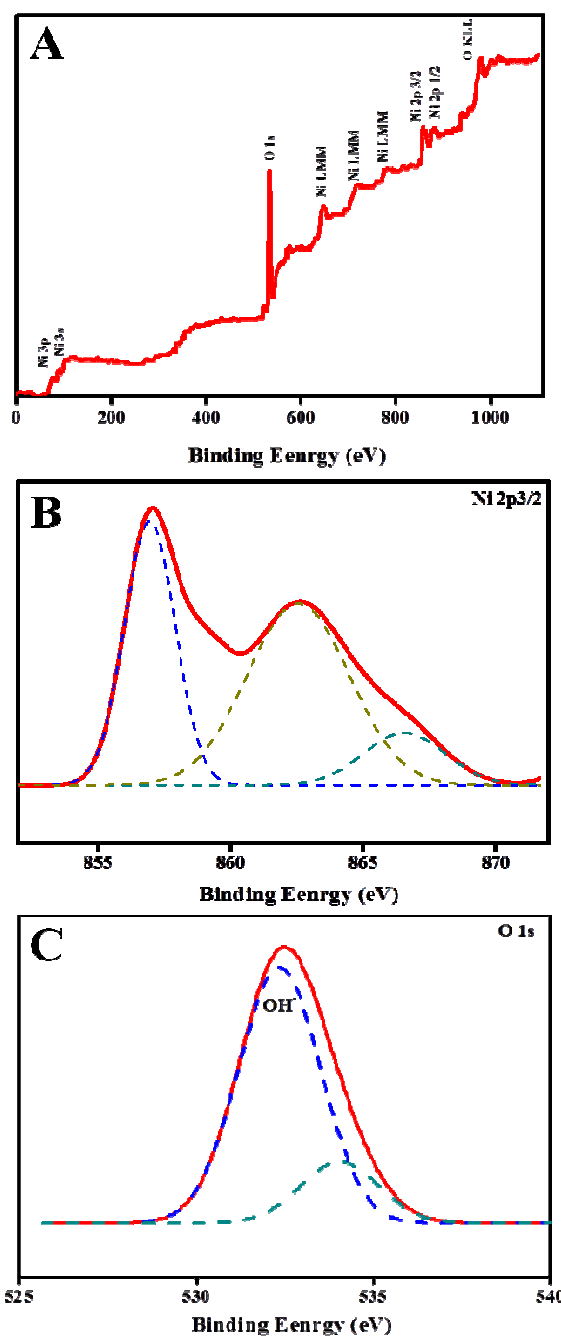

Fig.2

XPS spectra of survey scan (A), Ni2p3/2 (B), and O1s (C) regions in Ni(OH)$_2$ @ Cu dendrite

The bulk solution resistance R$_s$ and the electron-transfer resistance R$_{et}$ were obtained from the Nyquist plot. R$_{et}$ for the Ni(OH)$_2$@Cu dendrite was much smaller than that of Ni(OH)$_2$ film (Fig. 3, curve b) and similar to that of bare gold due to the high electric conductivity of the Cu dendrite core. The electrochemically active specific surface (S$_A$, cm^2 g^{-1}) [26, 35] can be calculated from the specific capacitance of the electrochemical double layer (C, Fg^{-1}) by means of the relationship S$_A$ = C/C$_d$, where C$_d$ is the capacitance of the electrochemical double layer, with a constant value of 20 mF cm^2. C is calculated from the EIS data in Fig. 3
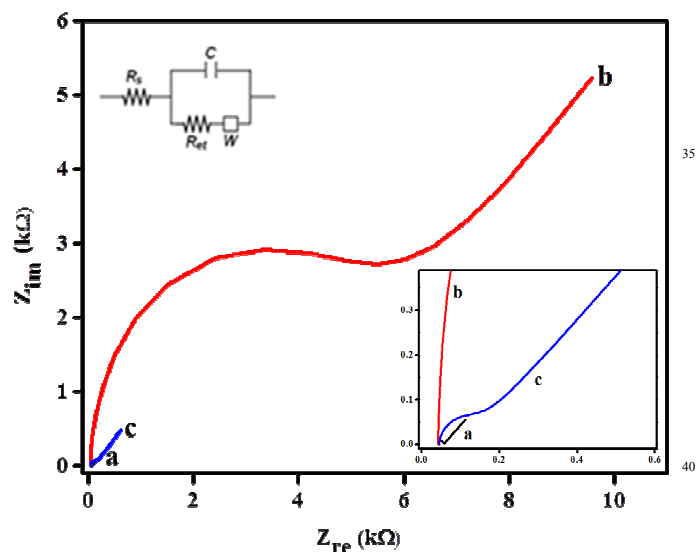
Electrode	R_{et} [ohmcm^{-2}]	C [Fg^{-1}]	S_A [cm^{2}g^{-1}]
Bare gold (a)	4 (±0.8)	0.02 (±0.004)	105
Ni(OH)$_2$ film (b)	1784 (±2.2)	0.06 (±0.009)	301
Ni(OH)$_2$ @ Cu dendrite (c)	6 (±0.6)	0.39 (±0.041)	1988

Fig. 3

Nyquist plots of bare gold (a), Ni(OH)$_2$ film (b), and Ni(OH)$_2$@Cu dendrite (c) in 0.1 M KCl containing 5 mM [Fe(CN)$_6$] and EIS data collected from bare gold, Ni(OH)$_2$ film, and Ni(OH)$_2$@Cu dendrite: R_{et}, C, and S_A represent the electron-transfer resistance, the double layer capacitance, and the surface area, respectively

The calculated specific surface area for the dendrite was 1988 cm^{2}g^{-1}, which was six times higher than that of the Ni(OH)$_2$ film (301cm^{2}g^{-1}). From these facts we could conclude that Ni(OH)$_2$@Cu dendrite structure was successfully prepared by a simple electro-depostion. The high surface area of the dendrite would allow the effective catalytic sites for electrochemical sensing.

Electrocatalytic oxidation of glucose at the Ni(OH)$_2$@Cu dendrite electrode

The electrocatalytic activities of the Ni(OH)$_2$@Cu dendrite, Ni(OH)$_2$ film, and Cu dendrite-modified electrode for glucose oxidation were investigated by cyclic voltammetry (CV) in 0.1 M NaOH containing 0.1 mM glucose (Fig 4A). All of the modified electrodes showed an oxidation peak at +0.6 V corresponding to the redox couple Ni(II)/Ni(III), which was responsible for the oxidation of glucose to glucolactone The sensing mechanism has already been reported in literature [10, 17, 18]. The results are in good agreement with those obtained by others [10, 17, 18, 29]. The Cu dendrite response current was fairly low. While the Ni(OH)$_2$@Cu dendrite electrode had a net current density. of 18.7 mAcm^{-2}, indicating that Ni(II)/Ni(III) was the main redox couple for glucose oxidation in the Ni(OH)$_2$@Cu dendrite.
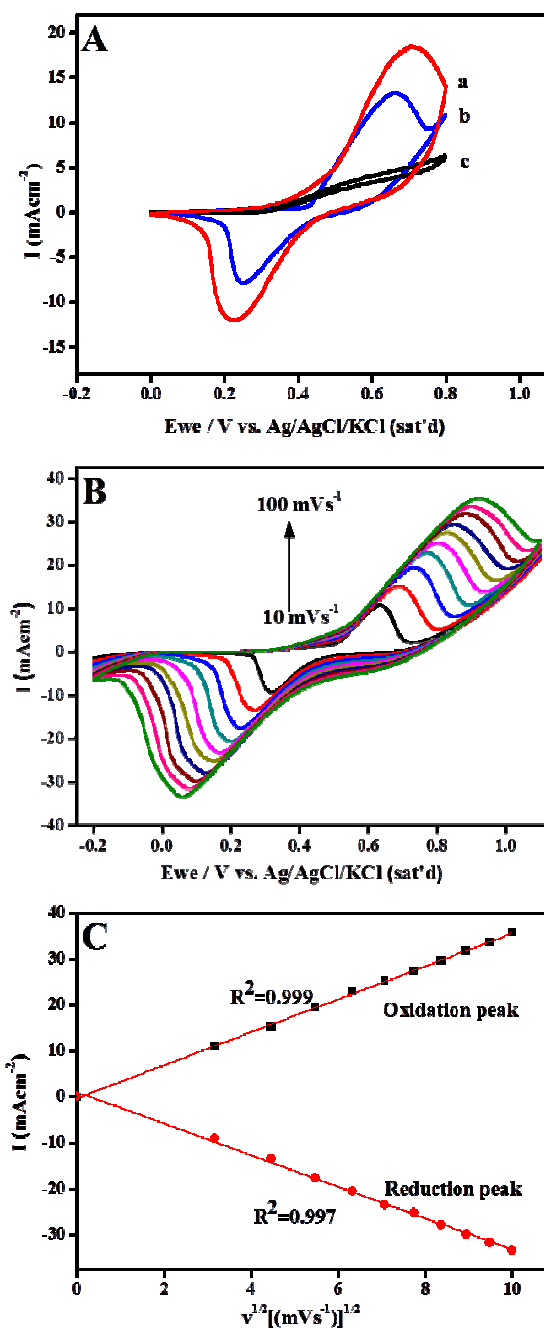

Fig. 4

A. CVs of Ni(OH)$_2$@Cu dendrite (a), Ni(OH)$_2$ film (b), and Cu dendrite (c) at a scan rate of 20 mV/s with 0.1 mM glucose/0.1 M NaOH solution

B. CVs of Ni(OH)$_2$@Cu dendrite at different scan rate from 10 to 100 mV/s with 0.1 mM glucose/0.1 M NaOH solution

C. Anodic and cathodic peak currents as a function of the square root of the scan rate

The anodic peak current at the Ni(OH)$_2$@Cu dendrite electrode was significantly higher than that of Ni(OH)$_2$ film (13.3 mAcm^{-2}). This indicates that the dendritic structure of the modified electrode provides a highly electro-active surface area of Ni(OH)$_2$. The CVs of the Ni(OH)$_2$@Cu dendrite electrode at various scan rates in the

range of 10 to 100 mVs⁻¹ are shown in Fig. 4B. With an increase in scan rate, the redox peak currents increased sharply, while oxidation and reduction peak potentials experienced positive and negative sides, resulting in a larger peak-to-peak separation. Both anodic and cathodic peak currents were directly proportional to the square root of scan rate (Fig. 4C), indicating a typical diffusion-controlled process, which suggested an ideal case for quantitative analysis in practical applications

Amperometric response of the Ni(OH)₂@Cu dendrite electrode for glucose detection

Chronoamperometry (CA) was used to measure the detection range, sensitivity, selectivity, reproducibility, and stability of the Ni(OH)₂@Cu dendrite electrode. In order to investigate the effect of applied potential on the signal, several potentials (+0.4, +0.5, +0.55, +0.6, and +0.65 V) were applied in order to monitor the amperometric response of the Ni(OH)₂@Cu dendrite to glucose detection. As shown in Figure S4 in the supplementary Materials, the modified electrode showed the best performance when the applied potential was +0.6 V. Hence, the subsequent CA analysis pertaining to glucose detection was conducted at +0.6 V. Figure 5A demonstrates the amperometric response to the successive addition of 1 μM, 5 μM, 10 μM, 0.1 mM, 0.5 mM (once every 100 s) spiked into 0.1 M NaOH solution for Ni(OH)₂@Cu dendrite and Ni(OH)₂ film electrode. The response time of the Ni(OH)₂@Cu dendrite and the Ni(OH)₂ film (achieving steady state current) was 2s and 7s. The response curve turns downward with increasing concentration. This is defined that an increasing amount of glucose is adsorbed onto the electrode surface, prolong the reaction time as shown in Fig.5A and 5B. From the calibration curves illustrated in Figure 5B, the Ni(OH)₂@Cu dendrite electrode provided a regression equation over a wide linear range of 1 μM - 4.5 mM, while the observed sensitivity was 2082 μAmM⁻¹cm⁻² (R² = 0.999) with a detection limit of 0.24 μM (S/N=3)[36]. The performances of the Ni(OH)₂@Cu dendrite and other non-enzymatic glucose sensors are compared in Table 1. Our sensor shows a higher sensitivity and wider linear range than the others. The anti-interference is another important parameter for a glucose sensor. The selectivity of the Ni(OH)₂@Cu dendrite electrode was tested by measuring the response to 1 mM glucose in the presence of electroactive species, such as urea, aspartic acid (AP), ascorbic acid (AA), dopamine (DP), and uric acid (UA), which are normally coexisted with glucose in human serum [37]. The normal physiological level of glucose is 4-7 mM, and the concentrations of other oxidative species are less than 0.1 mM, respectively [10]. The as prepared Ni(OH)₂ @ Cu dendrite was tested in successive addition of 1 mM glucose and 0.1 mM of other interfering species [38-39]. Figure 5C shows that negligible current responses were observed for the addition of interfering species as compared with adding glucose. These results indicated that the proposed Ni(OH)₂@Cu dendrite electrode can be used for the sensitive and selective detection of glucose in practical applications.
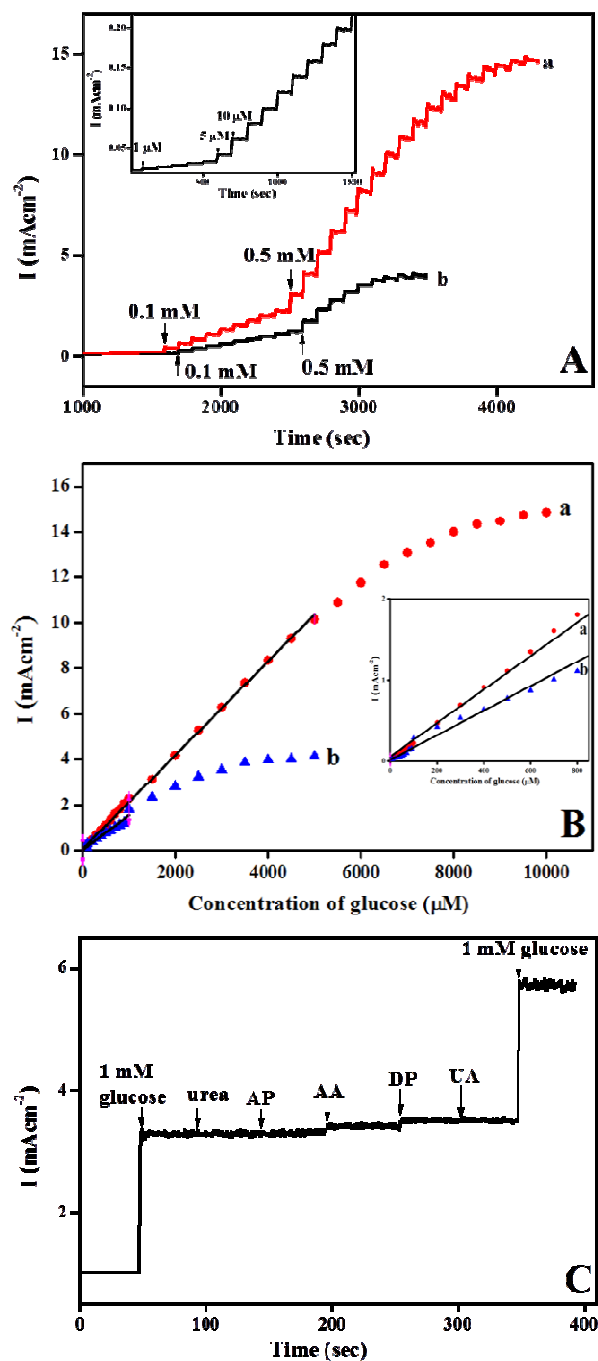

Fig. 5

A. Amperometric responses of Ni(OH)₂ @ Cu dendrite (a) and Ni(OH)₂ film (b) in 0.1 M NaOH with stepwise addition of glucose stock solution at applied potential: +0.6 V ; inset show the low concentration

B. Calibration curves of current response vs. glucose concentration with Ni(OH)₂ @ Cu dendrite (a) and Ni(OH)₂ film (b) ; inset show the low concentration

C. Amperometric response of Ni(OH)₂ @ Cu dendrite sensor in successive addition of 1 mM glucose and 0.1mM interferents (urea, AP, AA, DP, UA) in 0.1M NaOH at applied potential: +0.6V

Table 1. Performances of various non-enzyme glucose sensors

Sensors	Sensitivity ($\mu A \ mM^{-1}cm^{-2}$)	Linear range (μM)	Detection limit (μM)	Ref.
NiO/graphene	1571	5 - 2800	1	38
NiO-SWCNTs/ITO	907	1 - 900	0.3	39
Cu–NiO modified GCE	171.8	0.5 - 5000	0.5	28
Core−shell NiO/C nanobelts	149.11	0.1 - 170	9	40
Amorphous $Ni(OH)_2$ hollow nanoboxes	487.3	0.5 - 5000	0.07	15
$Ni(OH)_2$ nanoparticles	202	50 - 23000	6	18
RGO-$Ni(OH)_2$/GCE	11.43	2-3100	0.6	17
PI/CNT–$Ni(OH)_2$ nanospheres	2071.5	0.001 – 800	0.36	10
$Ni(OH)_2$ @ Cu dendrite	2082	1 - 4500	0.24	This work

Table 2. Determination of glucose in human urine samples

Sample	Subject	Urine (mM)	Spiked (mM)	$Ni(OH)_2$@Cu dendrite (mM)	HPLC (mM)	RSD (%) (n=3)	Recovery rate (%)
1	1	0.11	0.5	0.651	0.625	1.2	108.2
2	1	0.11	1	1.236	1.123	2.3	112.6
3	2	0.01	0.5	0.498	0.525	2.2	97.6
4	2	0.01	1	0.987	1.13	1.8	97.7

Real sample analysis

In order to further address the possible interference in glucose detection, the $Ni(OH)_2$@Cu dendrite electrode was used for the analysis of glucose spiked in human urine samples. All of urine samples were kindly supported by School of Medicine, Sungkyunwkan University: 55 year old male for subject 1 and 25 year old male for subject 2. The patients consented to the use of their samples in these experiments. Samples were diluted at a ratio of 1:2 (v/v) with 0.1 M NaOH and were stored at 4 ℃ with no other pre-treatments. Samples were diluted at a ratio of 1:2 (v/v) with 0.1 M NaOH and were stored at 4 ℃ with no other pre-treatments. Since glucose is not usually found in concentrations greater than 0.8 mM in urine from healthy people, the standard addition method was employed to spike 0.5 mM and 1 mM standard glucose solution into the samples [29]. The results shown in Table 2 clearly demonstrate that the concentrations detected by our sensor were in agreement with those measured by HPLC. Moreover, spike recoveries were found to be 97-108% with relative standard deviations (RSD) less than 3 % for three independent measurements. This suggests that the developed sensor can be used for the determination of glucose in human samples.

Reproducibility, repeatability, and stability

The reproducibility and repeatability of the developed dendrite sensor were also evaluated [41]. Five independent $Ni(OH)_2$@Cu dendrite probes were identically prepared in order to measure the amperometric responses to a 0.1 mM glucose solution, and a relative standard deviation (RSD) of 4.21 % was found. Five successive measurements of a 0.1 mM glucose solution using the same $Ni(OH)_2$@Cu dendrite probe yielded an RSD of 5.8 %. For long-term stability testing, the proposed sensor was stored in a desiccator at ambient conditions and then used to measure a 0.1 mM glucose solution once every week. After 70 days, the amperometric response of the sensor only decreased 4 % compared to the initial response. This result is attributed to both the structural and chemical stability of the $Ni(OH)_2$@Cu dendrite. These results indicated the $Ni(OH)_2$@Cu dendrite electrode can be used for glucose detection in a repeatable and reproducible manner without compromised sensing activity over time.

4. Conclusions

A novel $Ni(OH)_2$@Cu dendrite electrode was prepared by a facile two-step electrodeposition. The large effective surface area of the

dendrite structure promoted high charge-transfer and high biocompatibility. The electrocatalytic oxidation of this dendrite structure for glucose was found to be very efficient, achieving a high sensitivity of 2082 $\mu AmM^{-1}cm^{-2}$ and a detection limit of 0.24 μM. The designed electrode is competitive for the effective determination of glucose in a rapid, sensitive, and low-cost manner with little interference. The Ni(OH)$_2$@Cu dendrite electrode is a promising tool for the development of a non-enzymatic glucose determination.

Acknowledgements

Notes and references

[a] *School of chemical Engineering, Sungkyunkwan University, 440-746 Suwon, Republic of Korea. Fax: +82 31 299 4711; Tel: +82 31 290 7326; E-mail: yklee@skku.edu*

(1) J. Wang, *Chem. Rev.* 2008, **108**, 814 – 825

(2)   S. Peng, Y. Huang, T. Wang and J. Ma, *RSC Adv.*, 2013, **3**, 3487-3502.

(3) C. Chen, Q. Xie, D. Yang, H. Xiao, Y. Fu, Y. Tan and S. Yao, *RSC Adv.,* 2013, **3**, 4473–4491

(4) H. Nie, Z. Yao, X. Zhou, Z. Yang and S. Huang, *Biosens. Bioelectron.,* 2011, **30**, 28 – 34.

(5) F. Cao, S. Guo, H. Ma, D. Shan, S. Yang and J. Gong, *Biosens. Bioelectron.,* 2011, **26**, 2756 – 2760

(6) S. Park, T. D. Chung and H. Kim, *Anal. Chem.* 2003, **75**, 3046–3049

(7) B.K. Jena and C.R. Raj, *Chem. Eur. J.* 2006, **12**, 2702 – 2708

(8) H. Bai, M. Han, Y. Du, J. Bao and Z. Dai, *Chem. Comm.,* 2010, **46**, 1739 – 1741

(9) J. Zhu, J. Jiang, J. Liu, R. Ding, Y. Li, H. Ding, Y. Feng, G.Wei and X. Huang, *RSC Adv.,* 2011, **1**, 1020–1025

(10) Y. Jiang, S. Yu, J. Li, L. Jia and C. Wang, *Carbon* 2013, **63**, 367 – 375.

(11) S. Ci, T. Huang, Z. Wen, S. Cui, S. Mao, D.A. Steeber and J. Chen, *Biosens. Bioelectron.,* 2014, **54**, 251 – 257.

(12) H. Huo, C. Guo, G. Li, X. Han and C. Xu, *RSC Adv.,* 2014, **4**, 20459 – 20465

(13) Y. Mu, D. Jia, Y. He, Y. Miao and H.L. Wu, *Biosens. Bioelectron.,* 2011, **26**, 2948 – 2952.

(14) Y.J. Yang and S. Hu, *Electrochim. Acta,* 2010, **55**, 3471 – 3476.

(15)   J. Nai, S. Wang, Y. Bai and L. Guo, *Small* 2013, **9**, 3147 – 3152.

(16)   S. Zhou, X. Feng, H. Shi, J. Chen, F. Zhang and W. Song, *Sens.Actuators, B,* 2013, **177**, 445 – 452

(17) Y. Zhang, F. Xu, Y. Sun, Y. Shi, Z. Wen and Z. Li, *J. Mater. Chem.* 2011, **21**, 16949 – 16954.

(18) A. Safavi, N. Malekia and E. Farjamia, *Biosens. Bioelectron.,* 2009, **24**, 1655 – 1660.

(19) X.M. Yin, C.C. Li, M. Zhang, Q.Y. Hao, S. Liu, L.B. Chen and T.H. Wang, *J. Phys. Chem. C* 2010, **114**, 8084 – 8088

(20) F. Zhang, L. Hao, L.J. Zhang and X.G. Zhang, *Int. J. Electrochem. Sci.* 2011, **6**, 2943 – 2954.

(21) R. Qiu, X.L, Zhang, R. Qiao, Y. Li, Y.I. Kim and Y.S. Kang, *Chem. Mater.* 2007, **19**, 4174 – 4180.

(22) X. Zhang, G. Wang, W. Zhang, N. Hu, H. Wu and B. Fang, *J. Phys. Chem. C* 2008, **112**, 8856 – 8862.

(23) X. Niu, Y. Li, J. Tang, Y. Hu, H. Zhao and M. Lan, *Biosens. Bioelectron.,* 2014, **51**, 22 – 28.

(24) R. Qiu, H.G. Cha, H.B. Noh, Y.B. Shim, X.L. Zhang, R. Qiao, D. Zhang, Y.I. Kim, U. Pal and Y.S. Kang, *J. Phys. Chem. C* 2009, **113**, 15891 – 15896.

(25) T.H. Lin, C.W. Lin, H.H. Liu, J.T. Sheu and W.H. Hung, *Chem. Comm.,* 2011, **47**, 2044 – 2046.

(26) S.H. Lee, H. Lee, M.S. Cho, J.D. Nam and Y. Lee, *J. Mater. Chem. A* 2013, **1**, 14606 – 14611.

(27) D.J. Chen, Y.H. Lu, A.J. Wang, J.J. Feng, T.T. Huo and W.J. Dong, *J. Solid State Electrochem.* 2012, **16**, 1313 – 1321.

(28) X. Zhang, A. Gu, G. Wang, Y. Huang, H. Ji and B. Fang, *Analyst* 2011, **136**, 5175 – 5180

(29) J. Yang, J.H. Yu, J.Rudi Strickler, W.J. Chang and S. Gunasekaran, *Biosens. Bioelectron.,* 2013, **47**, 530 – 538.

(30) G.W. Yang, C.L. Xu and H.L. Li, *Chem. Comm.,* 2008, **48**, 6537-6539.

(31) J.W. Lee, T. Ahn, D. Soundararajan, J.M. Ko and J.D. Kim, *Chem. Comm.,* 2011, **47**, 6305 – 6307.

(32) H. B. Li, M. H. Yu, F. X. Wang, P. Liu, Y. Liang, J. Xiao, C. X. Wang, Y. X. Tong and G. W. Yang, *Nature Communications* 2013, **4**, 1894 – 1901.

(33) F. Muench, M. Oezasla, M. Rauber, S. Kaserer, A. Fuchs, E. Mankel, J. Brötz, P. Strasser, C. Roth and W. Ensinger, *J. Power sources,* 2013, **22**, 243 – 252.

(34) B.P. Payne, M.C. Biesinger and N.S. McIntyre, *J. Electron Spectrosc. Relat. Phenomena* 2012, **185**, 159 – 166.

(35) S.L. Chou, J.Z. Wang, H.K. Liu and S.X. Dou, *J. Power sources,* 2008, **182**, 359 – 364.

(36) M. Thosmpson and S.L. Ellison, *Pure Appl. Chem.* 2002, **74**, 835-855

(37) P. Si, Y. Huang, T. Wang and J. Ma, *RSC Advances, 2013, 3, 3487 – 3502*

(38) S.J. Li, N. Xia, X.L. Lv, M.M. Zhao, B. Q. Yuan and H. Pang, *Sens.Actuators, B,* 2014, **190**, 809 – 817.

(39) N.Q. Dung, D. Patil, H. Jung, J. Kim and D. Kim, *Sens. Actuators, B,* 2013, **183**, 381 – 387.

(40) D. Yang, P. Liu, Y. Gao, H. Wu, Y. Cao, Q. Xiao and H. Li, *J. Mater. Chem.* 2012, 22, 7224 – 7231

(41) X. Li, J. Yao, F. Liu, H. He, M. Zhou, N. Mao, P. Xiao and Y. Zhang, *Sens. Actuators, B,* 2013, 181, 501 – 508.